Proceedings of the 30th International Conference on Ocean, Offshore and Arctic Engineering OMAE2011 June 19-24, 2011, Rotterdam, The Netherlands

OMAE2011-49979

TOWARDS A GENERAL-PURPOSE OPEN BOUNDARY CONDITION FOR WAVE SIMULATIONS

Bulent Duz*
Department of Ship Hydrodynamics
Technical University of Delft
Mekelweg 2, 2628 CD Delft
The Netherlands
b.duz@tudelft.nl

Rene H.M. Huijsmans
Department of Ship Hydrodynamics
Technical University of Delft
Mekelweg 2, 2628 CD Delft
The Netherlands
r.h.m.huijsmans@tudelft.nl

Peter R. Wellens
Mart J.A. Borsboom
Deltares
P.O. Box 177, 2600 MH Delft
The Netherlands
(mart.borsboom, peter.wellens)@deltares.nl

Arthur E.P. Veldman
Institute for Mathematics and Computer Science
University of Groningen
P.O. Box 407, 9700 AK Groningen
The Netherlands
a.e.p.veldman@rug.nl

ABSTRACT

For the design of FPSO's in harsh environments an accurate assessment of the ability of the platform to survive in extreme sea conditions is of prime importance. Next to scaled model tests on the FPSO in waves also CFD capabilities are at the disposal of the designer. However even with the fastest computers available it is still a challenge to use CFD in the design stage because of the large computational resources they require. In that respect to use a small computational domain will improve the turn around time of the computations, however at the expense of various numerical artifacts, like reflection on artificial boundaries in the computational domain. In order to mitigate the reflection properties new absorbing boundary conditions have been developed. The work in this paper is constructed on the previous study about the generating and absorbing boundary condition (GABC) in the ComFLOW project. We present a method to apply the GABC on all the boundaries in a three dimensional domain. The implementation of the GABC in ComFLOW is explained in detail.

INTRODUCTION

Scientists and engineers regard the surface of the ocean as interesting due to one of the broadest physical phenomena which has been intensively studied in various fields of science: waves. Although waves can occur in all types amongst a variety depending on the forces acting on the water, one aspect exists in all the cases and attracts our attention: waves exert loads and stresses on numerous kinds of man-made structures in the ocean. If the other elements of the environment are also hostile, major catastrophic failures can appear threatening human safety and causing economic loss.

Most of the current techniques for investigating this complex problem generally fail to provide information beyond the point where particular numerical features of these techniques require focused and meticulous treatments. One of such numerical features is developing a robust and efficient boundary condition by means of which we can truncate the vast spatial domain , thus introducing a finite computational domain and a residual infinite domain. Following this step, we encounter two dominantly im-

*Address all correspondence to this author.

portant difficulties to overcome: the solution in the finite computational domain has to be unique, namely the boundary condition should not allow growing spurious modes to pollute the entire domain and, the amount of unwanted reflection from the boundary should be less than a specified threshold. Consequently, in order to improve the quality of the numerical solution, it is of fundamental importance to improve the properties of the boundary condition.

The Sommerfeld boundary condition [1] was the cornerstone of non-reflecting boundary conditions. Engquist and Majda [2,3] proposed a method to develop the first hierarchy of absorbing boundary conditions. Higdon [4] generalized this theory and showed that Engquist and Majda boundary condition is a subset of the Higdon operators. Since high order boundary operators include high order derivatives both in time and space, Collino and Joly [5] introduced the use of auxiliary variables to circumvent this problem. For a general review regarding high order local non-reflecting boundary conditions, see [6,7]. Although such local absorbing boundary conditions have been devised for approximately half a century, it is difficult to find a study in which the complexity of the free surface wave simulations in truncated domains have been thoroughly investigated. The difficulties regarding the boundary conditions mainly consist of dispersive and directional effects, transparency to incoming and outgoing waves at the same time, extra computational efforts associated with the boundary treatment, and efficiency requirements providing the opportunity to place the boundaries as close to the object in the computational domain as possible. Moreover the boundary condition has to be suitable for further improvements allowing the incorporation of nonlinear effects and the combination of flow current with the boundary condition. Since most of the above requirements are inherent to free surface wave simulations, a general absorbing boundary condition cannot be simply selected and utilized for our purposes.

The generating and absorbing boundary condition (GABC) is a result of a rare study [8] where various aspects of this subject are discussed. Here we shall focus our attention specifically on developing a method to apply the GABC in a three dimensional free surface wave simulation within the framework of ComFLOW. Numerical models employed in ComFLOW which is a volume-of-fluid (VOF) based Navier-Stokes solver employing a staggered grid arrangement are explained in full detail in [9 – 15].

STATEMENT OF THE PROBLEM

In the previous model, GABC is applied on the west boundary Γ_W which allows the incoming wave to enter the domain while letting the outgoing wave to leave the domain. Thus a fully transparent boundary condition is employed at the inflow boundary of the computational domain as illustrated in Fig. 1(a). On the east boundary Γ_E, an absorbing boundary condition (ABC) is stipulated which allows the outgoing waves to exit the computational domain. On the north and south boundaries Γ_N, Γ_S a wall boundary condition is implemented. By means of all the boundary conditions a three-dimensional unbounded medium is truncated along x and y direction resulting in a finite computational domain in which wave-structure interaction problems are numerically solved. In case of an obstacle in the domain the problem would be similar to a time dependent scattering problem and the reflected waves from the object would propagate in all the directions. North and south boundaries reflect the waves fully back into the domain, as a result spoil the solution everywhere. In order to set-up a computational domain in which absorbing boundary conditions are stipulated on all the boundaries, mainly two approaches arise in terms of specifying the angle between the direction of the wave propagation and the boundaries of the domain. They are depicted in Fig. 1. In Fig. 1(a) GABC

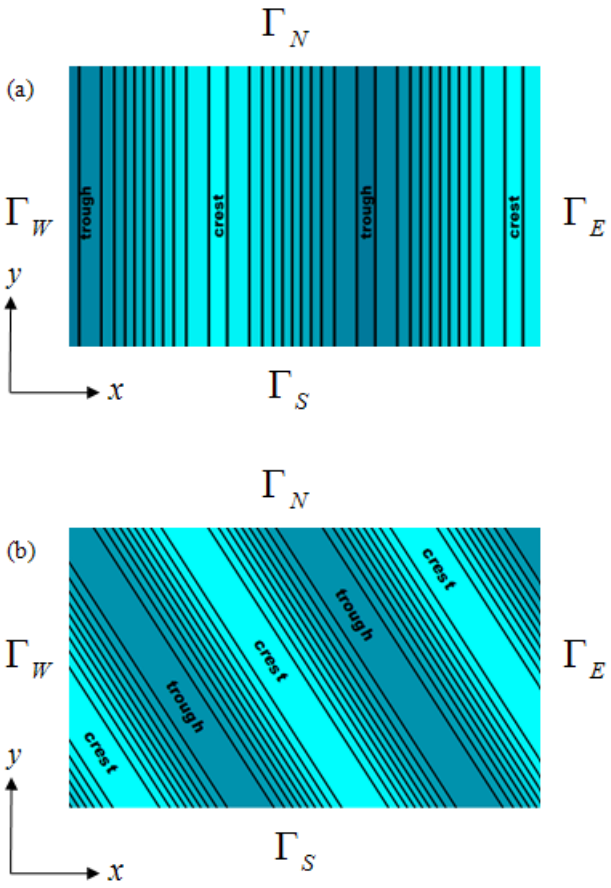

FIGURE 1. WAVE PATTERNS IN DIFFERENT DOMAINS (TOP VIEW): (a) WAVES PROPAGATING PARALLEL TO THE BOUNDARIES and (b) WAVES PROPAGATING UNDER AN ANGLE.

at the inflow Γ_W and ABC on the remaining boundaries Γ_N, Γ_S, and Γ_E are specified. In this situation although the implementation is rather simple we encounter some problems regarding the wave profile and the reflection property since waves propagate parallel to north and south boundaries along x direction. In close vicinity of the north and south boundaries wave crests appear to be distorted. For a brief discussion about the results of this approach see [16]. In Fig. 1(b) waves are sent into the computational domain under an angle, thus removing the possibility of parallel propagation completely. Here GABC is prescribed on Γ_W and Γ_S introducing them as inflow boundaries while ABC is prescribed on Γ_N and Γ_E introducing them as outflow boundaries. From this point on we will restrict ourselves to the latter approach.

MATHEMATICAL FORMULATION

In a locally homogeneous medium, a plane wave which shows a periodic behavior both in space and time presents the form of the solution to a scalar wave equation. If $\phi(x_i,t)$ denotes a field variable such as pressure or velocity

$$\phi(\vec{x},t) = \phi(x_i,t) = \mathrm{Re}\left[Ae^{i(\vec{k}.\vec{x}-\omega t)}\right] \tag{1}$$

$$\phi(x_i,t) = |A|\cos\left(\vec{k}.\vec{x} - \omega t + \tan^{-1}\frac{\mathrm{Im}A}{\mathrm{Re}A}\right) \tag{2}$$

where A is the complex wave amplitude, $\vec{k}$ is the wave vector, ω is the wave frequency and Re indicates the real part of the expression. For a plane wave propagating in the direction of an arbitrary wave vector in $x-y$ space, such as illustrated in Fig. 2, we have

$$\begin{aligned} \vec{k} &= k_x i + k_y j \\ k_x &= \left|\vec{k}\right|\cos\theta \\ k_y &= \left|\vec{k}\right|\sin\theta \end{aligned} \tag{3}$$

The phase speed in x-direction can be defined such that at fixed y,

$$d\left(\left|\vec{k}\right|\cos\theta dx - \omega dt\right) = 0 \tag{4}$$

$$c_x = \frac{dx}{dt} = -\frac{\partial\left(\left|\vec{k}\right|\cos\theta dx - \omega dt\right)/\partial t}{\partial\left(\left|\vec{k}\right|\cos\theta dx - \omega dt\right)/\partial x} = \frac{\omega}{\left|\vec{k}\right|\cos\theta} \tag{5}$$

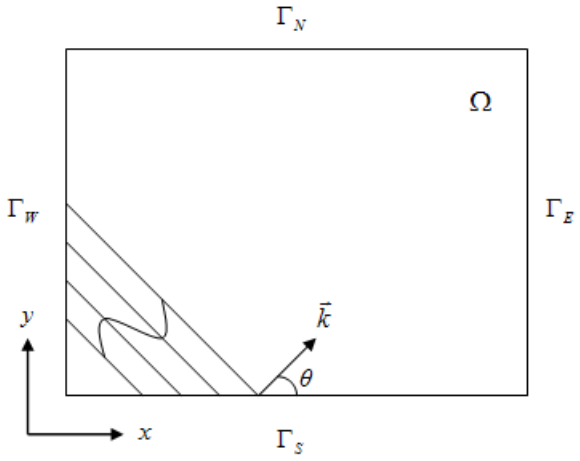

FIGURE 2. A TRAVELING PLANE WAVE WITH AN ANGLE OF INCIDENCE (TOP VIEW).

Substituting the definition of the phase speed, $c = \omega/\left|\vec{k}\right|$, into Eqn. (5) yields the following expression for the phase speed in the x-direction,

$$c_x = \frac{c}{\cos\theta} \tag{6}$$

Note that c_x is not a vector. Pursuing the same understanding the phase speed in the y-direction would be found as,

$$c_y = \frac{c}{\sin\theta} \tag{7}$$

If we substitute Eqn. (6) and Eqn. (7) into the Sommerfeld boundary condition [1] for a plane wave traveling out of Ω with an angle of incidence θ as shown in Fig. 2, we reach a first order Higdon [4] operator which can also be considered as a first order Engquist-Majda [2] operator by setting $\alpha = 0^\circ$

$$\left(\frac{\partial}{\partial t} + \frac{c^{out}}{\cos\alpha}\frac{\partial}{\partial x}\right)\Phi^{out} = 0 \tag{8}$$

$$\left(\frac{\partial}{\partial t} + \frac{c^{out}}{\sin\alpha}\frac{\partial}{\partial y}\right)\Phi^{out} = 0 \tag{9}$$

for $|\alpha| < \pi/2$. The difference between θ and α is that while θ is the actual angle under which waves are propagating, α can be regarded as a prespecified boundary condition parameter. Eqn. (8)

is prescribed on Γ_E while Eqn. (9) is prescribed on Γ_N. The following discussion regarding the reflection coefficient is associated with the boundary operator on Γ_E. If we denote the total wave signal at the boundary as the superposition of an outgoing wave with amplitude normalized to one, and an incoming spuriously reflected wave with amplitude R being the reflection coefficient, we can take

$$\begin{aligned}\Phi &= e^{i\left(|\vec{k}|\cos(\theta)x+|\vec{k}|\sin(\theta)y-\omega t\right)} \\ &+Re^{i\left(-|\vec{k}|\cos(\theta)x+|\vec{k}|\sin(\theta)y-\omega t\right)}\end{aligned} \tag{10}$$

Since the choice of α is arbitrary, in general for any linear combination of plane waves propagating in the direction of $\vec{k}$ with phase speed c^{out}, the reflection coefficient depends on the angle of incidence θ and the specified value for α,

$$R = -\frac{\cos(\alpha)-\cos(\theta)}{\cos(\alpha)+\cos(\theta)} \tag{11}$$

If α is selected to be equal to the angle of incidence θ the boundary operator provides perfect absorption. Regardless of the values of α, R has an absolute value less than 1 when $|\theta| < \pi/2$. If the wave has components traveling with phase speeds different than c^{out} then there will appear another source of reflection. In this situation the reflection coefficient can be determined as,

$$R = \frac{c^{out}\cos\theta - c(kh)\cos\alpha}{c^{out}\cos\theta + c(kh)\cos\alpha} \tag{12}$$

where $c(kh)$ is the actual phase speed of the wave component impinging on the boundary. In Eqn. (12) both the effect of the angle of incidence and the effect of different phase speeds are taken into account. It is clear that possessing information a priori regarding only phase speed or wave direction is not enough for tolerable reflection since both of the parameters contribute to the amount of reflection.

In order to derive a boundary condition which has a feature of generating reflection up to an acceptable limit for all wave components one can follow numerous approaches one of which is exploiting high order boundary operators. Since they contain high order derivatives both in time and space an alternative method is preferred here.

$$c = \sqrt{gh}\sqrt{\frac{\tanh(kh)}{kh}} \tag{13}$$

$$c_a \approx \sqrt{gh}\frac{a_0 + a_1(kh)^2}{1 + b_1(kh)^2} \tag{14}$$

Following the procedure described in [8], we introduce a rational approximation (14) to the dispersion relation (13) where $\sqrt{gh}$ denotes the shallow water phase speed and kh denotes the dimensionless wave number. Here the idea is to replace the dispersion relation by an expression which proposes an accurate approximation to be substituted in a boundary condition for wave components traveling with different phase speeds. Parameters in (14) have to be chosen so that it is accurate for the largest possible range of kh values. However, individual wave numbers pertaining to individual wave components are not incorporated into (14) due to the fact that only a single wave number appears in the approximation. To overcome this difficulty individual wave numbers are resolved from the solution variable Φ^{out} using the relation

$$k^2\Phi^{out} = \frac{\partial^2}{\partial z^2}\Phi^{out} \tag{15}$$

When (14) and (15) are written in (8), the final form of the boundary condition to be applied on Γ_E for dispersive waves becomes

$$\left[\left(1 + b_1h^2\frac{\partial^2}{\partial z^2}\right)\cos\alpha\frac{\partial}{\partial t} + \sqrt{gh}\left(a_0 + a_1h^2\frac{\partial^2}{\partial z^2}\right)\frac{\partial}{\partial x}\right]\Phi^{out} = 0 \tag{16}$$

Replacing c^{out} in (12) by (14) to find the reflection coefficient for (16) results in

$$R = \frac{\sqrt{gh}\left(a_0 + a_1(kh)^2\right)\cos\theta - c(kh)\left(1 + b_1(kh)^2\right)\cos\alpha}{\sqrt{gh}\left(a_0 + a_1(kh)^2\right)\cos\theta + c(kh)\left(1 + b_1(kh)^2\right)\cos\alpha} \tag{17}$$

The main advantages of the boundary condition given in (16) are as follows

- Eqn. (16) provides a general form which is easily applicable for dispersive wave problems in two and especially in three dimensions without increasing the computational load substantially. This feature evidently brings the possibility to truncate the domain not only on x-direction but also on y-direction which reduces the computational efforts significantly.
- It is obvious to see that the character of the absorbing boundary condition does not stipulate any dependency on phase speed or wave number because they are computed via the solution variable Φ^{out}. Moreover one has the opportunity to investigate various sea states by changing the parameters in (14) where an accurate approximation for a range of kh values is implemented.
- If there is an offshore structure in the domain, which in practice there is, it would be interesting to study the effect

of the angle of incidence on the wave loading exerted on the structure. In the current model this is delivered since the direction of wave propagation is accounted for.

∗ When the total wave signal at the inflow boundary is decomposed as $\Phi = \Phi^{in} + \Phi^{out}$, then it is straightforward to substitute this relation in (16) to achieve a boundary condition which is fully transparent allowing waves to penetrate into the domain and also to move out of the domain.

∗ Comparing the reflection coefficients given in (11), (12) and (17), the latter provides more control over the reflection property of the boundary condition. For appropriately prespecified values of the parameters in (17), the spurious reflection from the boundary will become small for a region in the vicinity of a kh value. This is a consequence of the fact that an accurate approximation for the dispersion relation (13) is posed via (14) over that region.

NUMERICAL IMPLEMENTATION

Comflow solves the Navier-Stokes equations in terms of primitive variables, namely velocity components and pressure. Therefore we need to interpret (16) by means of the same variables. Exploiting the Bernoulli equation and potential theory, it is possible to achieve the following relations

$$\frac{\partial \Phi}{\partial t} = -\frac{p_b}{\rho} - g z_p \tag{18}$$

$$\frac{\partial \Phi}{\partial x} = u_b \tag{19}$$

Here p_b represents the pressure value at the domain boundary which is situated along the x-position of u_b denoting x-component of velocity at the boundary. Since a staggered grid arrangement is employed for the solution variables inside cells as can be seen in Fig. 3, we will use mirror cells outside the domain to interpolate the pressure over the boundary Γ_E. The shaded areas in Fig. 3 contain the mirror cells which have indices $(0,k)$ adjacent to inflow and $(I+1,k)$ adjacent to outflow for $k = 1,...,K$ in $x-z$ domain. By combining (16), (18) and (19), we obtain the final form of the ABC

$$\begin{aligned}
&\left[\tfrac{1}{2}\cos\alpha + \beta\tfrac{\Delta t}{\Delta x_{p(I+1,k)}} + \left(\chi + a_1 h^2\sqrt{gh}\tfrac{\Delta t}{\Delta x_{p(I+1,k)}}\right)\tfrac{\partial^2}{\partial z^2}\right] p^{n+1}_{I+1,k} \\
&+ \left[\tfrac{1}{2}\cos\alpha - \beta\tfrac{\Delta t}{\Delta x_{p(I+1,k)}} + \left(\chi - a_1 h^2\sqrt{gh}\tfrac{\Delta t}{\Delta x_{p(I+1,k)}}\right)\tfrac{\partial^2}{\partial z^2}\right] p^{n+1}_{I,k} \\
&= \left(\beta + a_1 h^2\sqrt{gh}\tfrac{\partial^2}{\partial z^2}\right)\tilde{u}^n_{I,k} - g z_{p(I+1,k)}\cos\alpha
\end{aligned} \tag{20}$$

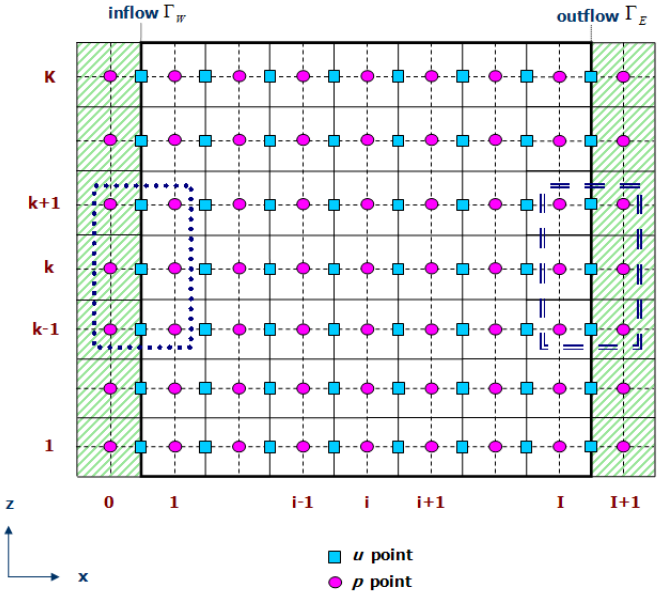

FIGURE 3. STENCILS USING A STAGGERED GRID ARRANGEMENT IN $x-z$ DOMAIN.

$$\begin{aligned}
&\left[\tfrac{1}{2}\cos\alpha + \beta\tfrac{\Delta t}{\Delta x_{p(0,k)}} + \left(\chi + a_1 h^2\sqrt{gh}\tfrac{\Delta t}{\Delta x_{p(0,k)}}\right)\tfrac{\partial^2}{\partial z^2}\right] p^{n+1}_{0,k} \\
&+ \left[\tfrac{1}{2}\cos\alpha - \beta\tfrac{\Delta t}{\Delta x_{p(0,k)}} + \left(\chi - a_1 h^2\sqrt{gh}\tfrac{\Delta t}{\Delta x_{p(0,k)}}\right)\tfrac{\partial^2}{\partial z^2}\right] p^{n+1}_{1,k} \\
&= \left(\beta + a_1 h^2\sqrt{gh}\tfrac{\partial^2}{\partial z^2}\right)\tilde{u}^n_{0,k} - g z_{p(0,k)}\cos\alpha + \Psi^{in}
\end{aligned} \tag{21}$$

where

$$\begin{aligned}
\Psi^{in} &= \left[\left(1 + b_1 h^2\tfrac{\partial^2}{\partial z^2}\right)\cos\alpha\tfrac{\partial}{\partial t} + \sqrt{gh}\left(a_0 + a_1 h^2\tfrac{\partial^2}{\partial z^2}\right)\tfrac{\partial}{\partial x}\right]\Phi^{in} \\
\chi &= \tfrac{1}{2} b_1 h^2\cos\alpha \\
\beta &= a_0\sqrt{gh} \\
\rho &= 1 \\
\Delta x_{p(I+1,k)} &= x_{p(I+1,k)} - x_{p(I,k)}
\end{aligned} \tag{22}$$

We notice that (20) and (21) involve pressure points at the new time step on the left and x-component of velocity at the old time step on the right. The x-component of velocity at the new time step arising from the relation in (19) is eliminated via the (discrete) x-momentum equation as described in [8] and [17]. Although we have $P^{n+1}_{(I,k)}$ in (20), since it is located within the domain boundaries, the ABC is in fact designed for $P^{n+1}_{(I+1,k)}$ which resides in the shaded area outside the domain. For $P^{n+1}_{(I+1,k)}$ the stencil of (20) encompassing 9 solution values is plotted in Fig. 3 using a double dashed line. The stencil for $P^{n+1}_{(0,k)}$ is plotted using a single dotted line. Note that the stencil is exactly the same as for $P^{n+1}_{(I+1,k)}$ leading us to the conclusion that the additional term on the right hand side of the boundary condition on Γ_W (21) does

not introduce extra entities in the coefficient matrix. In (21) Ψ^{in} represents the incoming wave which is known in advance. From (20) and (21) it is rather simple to obtain the boundary conditions for Γ_S and Γ_N.

RESULTS AND CONCLUSION

We apply the dispersive GABC to a problem in three dimesions where a fifth-order Stokes wave is sent into the computational domain under an angle of incidence (See Fig. 2 for a depiction of the problem). Here Γ_W and Γ_S are defined as inflow boundaries on which we apply the dispersive GABC whereas on Γ_N and Γ_E we apply the dispersive ABC. For a fifth-order Stokes wave we possess the exact values of the solution variables, namely velocity components, pressure and free surface elevations. We compare the theoretical and numerical results by

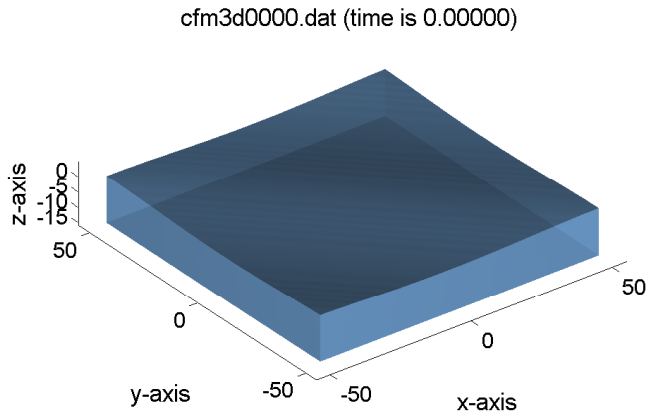

FIGURE 4. INITIAL CONDITION FOR THE NUMERICAL SIMULATION.

introducing two error measures. The first one is the pointwise error at a single point (i, j, K) in Ω which we will utilize to plot the difference between the free surface elevations of two calculations, i.e.,

$$e(i,j,K) = \eta_\Omega(i,j,K) - \eta_E(i,j,K) \tag{23}$$

for $i = 1,...,I$ and $j = 1,...,J$. The second error measure is the Eulerian norm of the error over each line in z-direction which we will use to plot the difference between the velocity values of two simulations,i.e.,

$$E(i,j,K) = \sqrt{\frac{1}{K}\sum_{k=1}^{K}\left(p_\Omega(i,j,k) - p_E(i,j,k)\right)^2} \tag{24}$$

for $i = 1,...,I$, $j = 1,...,J$ and $k = 1,...,K$.

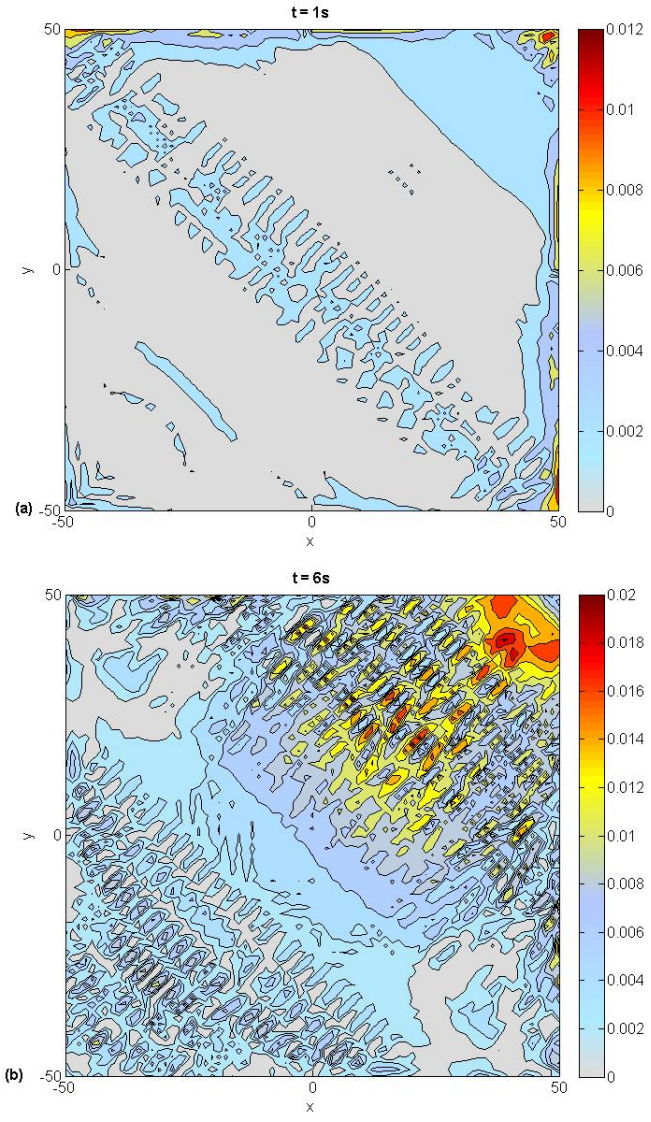

FIGURE 5. THE DIFFERENCE BETWEEN THE WAVE ELEVATIONS OF THE NUMERICAL AND THEORETICAL SIMULATION. ERRORS ARE SHOWN AT TIMES: (a) t=1s, (b) t=6s.

In Fig. 4 the initial condition pertaining to the ComFLOW

simulation of the fifth-order Stokes wave is given. The initial condition is an undisturbed wave profile, therefore errors equal to zero at the beginning of the simulation. The domain

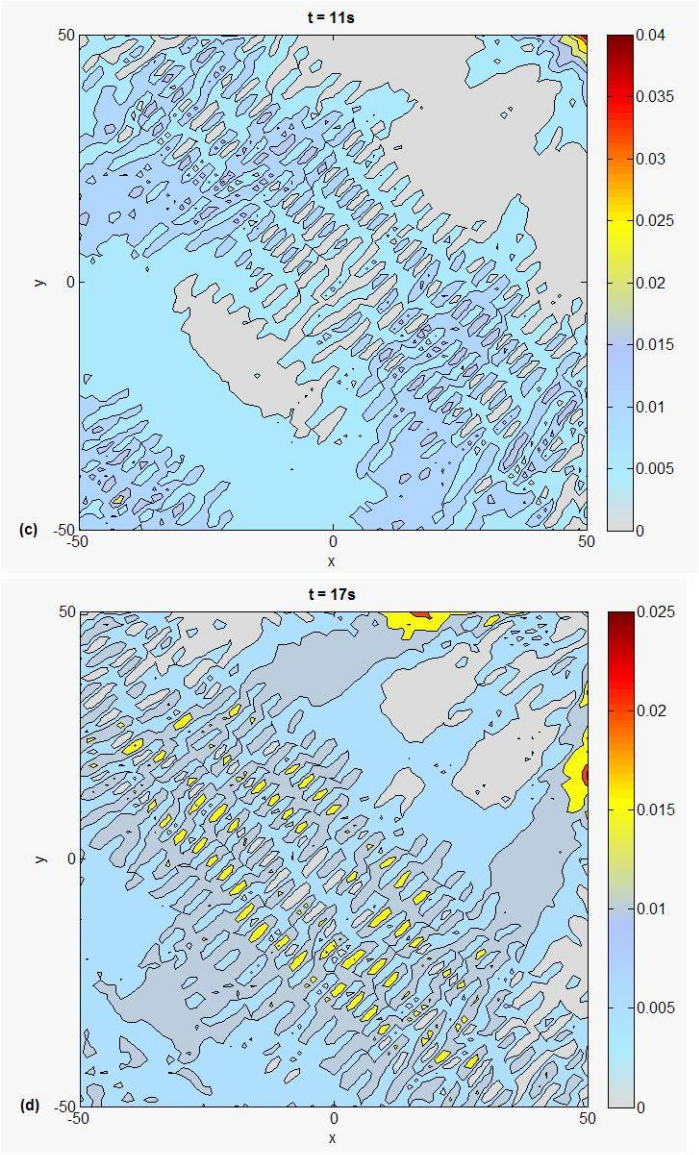

FIGURE 6. (CONTINUED FROM Fig. 5). ERRORS ARE SHOWN AT TIMES: (c) t=11s, (d) t=17s.

length in x- and y-direction is the same, $l_x = l_y = 100m$ whereas $l_z = 19m$ with the water depth $h = 15m$. The grid resolution is $\Delta x \times \Delta y \times \Delta z = 1.3m \times 1.3m \times 0.38m$, with 5% vertical stretching near the free surface. A fifth-order Stokes wave (wave period $T = 7.5s$, wave height $H = 1.3m$, wave length $\lambda = 74.7m$, phase speed $c = 9.97m/s$) is simulated by performing 2428 time-steps at $\Delta t = 0.007s$. The angle between the wave direction and the positive x-axis is 45°. Pointwise errors corresponding to the difference between the free surface elevations of two simulations at time $t = 1s$, $t = 6s$, $t = 11s$ and $t = 17s$ are demonstrated in Figs. 5 and 6. The amplitudes of the errors do not change substantially in time but the errors penetrate the interior. This result is indeed a manifestation of the fact that the reflected waves from the boundary travel back and perturb the solution in the entire computational domain. Since the absorbing boundary scheme

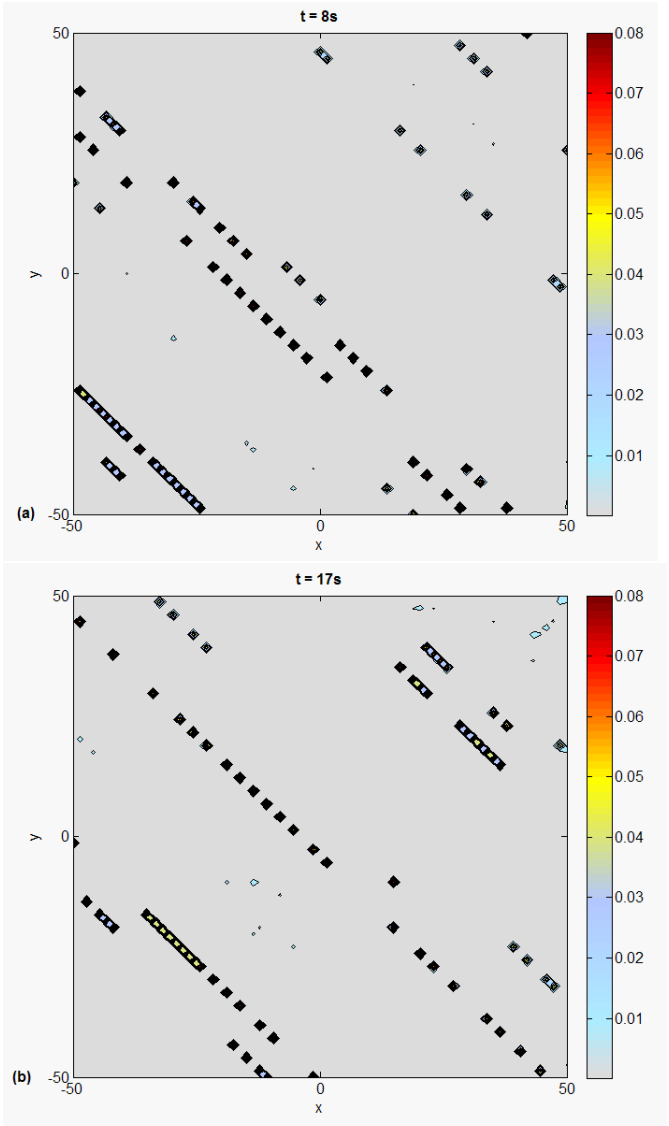

FIGURE 7. THE EULERIAN NORM OF THE ERROR FOR THE Z-COMPONENT OF THE VELOCITY. ERRORS ARE SHOWN AT TIMES: (a) t=8s, (b) t=17s.

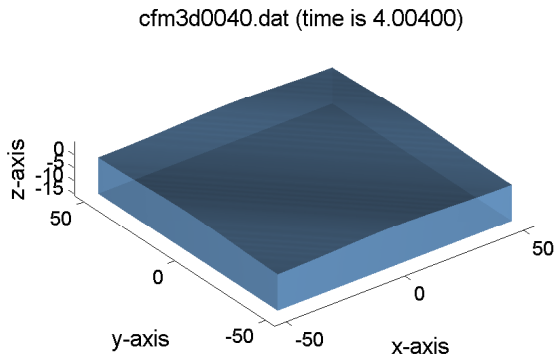

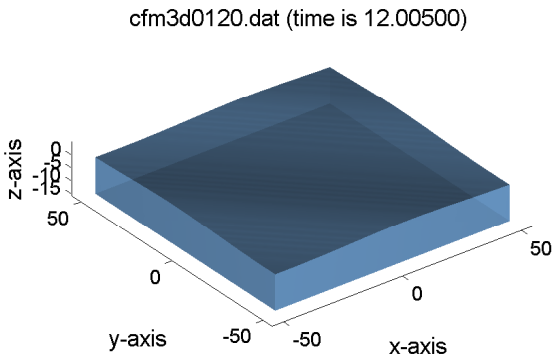

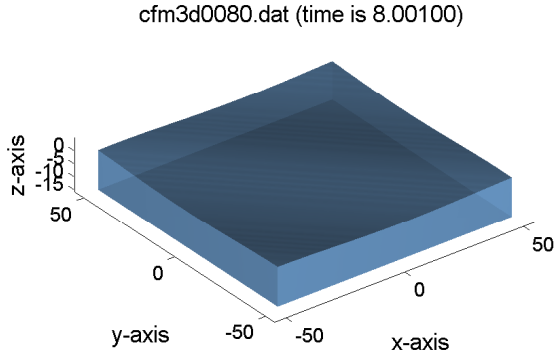

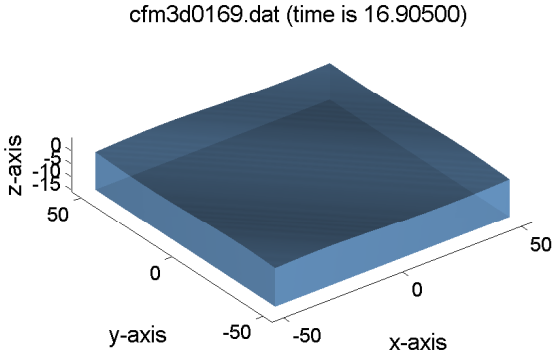

FIGURE 8. SNAPSHOTS OF A FIFTH-ORDER STOKES WAVE. FIGURES ARE SHOWN AT TIMES: t=4.0s, t=8.0s.

FIGURE 9. (CONTINUED FROM Fig. 8). FIGURES ARE SHOWN AT TIMES: t=12.0s, t=16.9s.

causes reflection to some extent as it is the case for other non-reflecting boundary models, the accumulation of the error in time becomes inevitable. Observing Figs. 5 and 6 we realize that the parts of the domain where the largest errors reside grow in time although very slowly. Fig. 7 illustrate the Eulerian norm of the error generated by the difference of the z-component of the velocity values in two calculations. Note that in order to examine the error quantitatively and globally, we use $E(i,j,K)$ instead of $e(i,j,K)$ over each line along the water depth, namely the z- direction because, as Figs. 5 and 6 evidently show, the reflected waves move backwards in the domain and the errors are not located just on the boundaries but everywhere. Snapshots of the simulation at different time instances are shown in Figs. 8 and 9.

One of the reasons for the aforementioned consequences is the mesh size. In order to grasp the physics of the problem more accurately, a well and densely constructed grid is needed especially within the vicinity of the free surface where the velocity and pressure gradients are significantly large. For especially high waves, the number of cells in the wave height and the wave length has to be increased. However, this will increase the computational costs substantially. A possible remedy for this issue can be to decrease the domain size however at the expense of the fact that in small domains reflected waves reach the remote locations in shorter times and the error accumulates more rapidly. Therefore, for a small domain the simulation time should be short, e.g., one wave period or less, but for sufficiently large domains longer simulations can be preferred. It should also be mentioned that during the development process of the boundary condition we have used a number of approximations based on the linear theory, but since the traveling waves in the computational domain are high-order Stokes waves, the additional terms arising from the Stokes theory contribute to the amount of reflection.

Consequently, the ABC which we applied in a free surface wave simulation in three dimensions demonstrated a good performance. The numerical results are in reasonable agreement with the theoretical calculation although the grid can be consid-

ered as coarse for a wave simulation. Related future work will include the implementation of the proposed absorbing boundary scheme to higher order boundary operators within the framework of ComFLOW.

ACKNOWLEDGMENT

The research is supported by the Dutch Technology Foundation STW, applied science division of NWO and the technology programma of the Ministry of Economic Affairs in The Netherlands (contracts GWI.6433 and 10475).

REFERENCES

[1] Sommerfeld, A., 1949. "Partial differential equations in physics". Academic Press.

[2] Engquist, B. and Majda, A., 1977. "Absorbing boundary conditions for the numerical simulation of waves". *Math. Comput.*, **31**, pp. 629-651

[3] Engquist, B. and Majda, A., 1977. "Absorbing boundary conditions for numerical simulation of waves". *Proc. Natl. Acad. Sci. USA*, **74**, pp. 1765-1766

[4] Higdon, R. L., 1987. "Numerical absorbing boundary conditions for the wave equation". *Math. Comput.*, **49**, 65-90.

[5] Collino, F. and Joly, P., 1995. "New absorbing boundary conditions for the finite element solution of 3D Maxwell's equations". *IEEE. Transactions on Magnetics*, **31(3)**, 1696-1701.

[6] Givoli, D., 1991. "Non-reflecting boundary conditions: a review". *J. Comput. Phys.*, **94**, pp. 1-29

[7] Givoli, D., 2004. "High-order local non-reflecting boundary conditions: a review". *Wave Motion*, **39**, pp. 319-326

[8] Wellens, P., 2011. "Wave simulations in truncated domains for offshore applications". PhD Thesis, Technical University of Delft, The Netherlands.

[9] Veldman, A.E.P., Luppes, R., Bunnik, T., Huijsmans, R.H.M., Duz, B., Iwanowski, B., Wemmenhove, R., Borsboom, M.J.A., Wellens, P.R., van der Heiden, H.J.L., van der Plas, P., 2011. "Extreme wave impact on offshore platforms and coastal constructions". In Proc. 30th Conf. on Ocean, Offshore and Arctic Engineering OMAE2011. Paper OMAE2011-49488

[10] Kleefsman, K. M. T., Fekken, G., Veldman, A. E. P., Iwanowski, B., and Buchner, B., 2005. "A Volume-of-Fluid based simulation method for wave impact problems". *J. Comput. Phys.*, **206**, pp. 363393.

[11] Veldman, A. E. P., Gerrits, J., Luppes, R., Helder, J. A., and Vreeburg, J. P. B., 2007. "The numerical simulation of liquid sloshing on board spacecraft". *J. Comput. Phys.*, **224**, pp. 8299.

[12] Gerrits, J., 2001. "Dynamics of Liquid-Filled Spacecraft". PhD Thesis, University of Groningen, The Netherlands.

[13] Fekken, G., 2004. "Numerical simulation of free-surface flow with moving objects". PhD Thesis, University of Groningen, The Netherlands.

[14] Kleefsman, K. M. T., 2005. "Water impact loading on offshore structures - a numerical study". PhD Thesis, University of Groningen, The Netherlands.

[15] Wemmenhove, R., 2008. "Numerical simulation of two-phase flow in offshore environments". PhD Thesis, University of Groningen, The Netherlands.

[16] Duz, B., 2010. "Extending the GABC to three-dimensions in ComFLOW". Comflow Report, unpublished.

[17] Wellens, P. R., Luppes, R., Veldman, A. E. P., and Borsboom, M. J. A., 2009. "CFD simulations of a semi-submersible with absorbing boundary conditions". In Proc. 28th Conf. on Ocean, Offshore and Arctic Eng. OMAE2009. Paper OMAE200979342.